Available online at www.sciencedirect.com

ScienceDirect

www.elsevier.com/locate/jes

JES JOURNAL OF ENVIRONMENTAL SCIENCES

www.jesc.ac.cn

Fatty acid fouling of forward osmosis membrane: Effects of pH, calcium, membrane orientation, initial permeate flux and foulant composition

Pin Zhao[1], *Baoyu Gao*[1], *Qinyan Yue*[1,*], *Pan Liu*[1], *Ho Kyong Shon*[2]

1. *Shandong Provincial Key Laboratory of Water Pollution Control and Resource Reuse, School of Environmental Science and Engineering, Shandong University, Jinan 250100, China*
2. *School of Civil and Environmental Engineering, University of Technology, Sydney, Broadway, NSW 2007, Australia*

ARTICLE INFO

Article history:
Received 10 July 2015
Revised 11 December 2015
Accepted 17 February 2016
Available online 18 March 2016

Keywords:
Forward osmosis
Membrane fouling
Octanoic acid
Water flux
Reverse solute flux

ABSTRACT

Octanoic acid (OA) was selected to represent fatty acids in effluent organic matter (EOM). The effects of feed solution (FS) properties, membrane orientation and initial permeate flux on OA fouling in forward osmosis (FO) were investigated. The undissociated OA formed a cake layer quickly and caused the water flux to decline significantly in the initial 0.5 hr at unadjusted pH 3.56; while the fully dissociated OA behaved as an anionic surfactant and promoted the water permeation at an elevated pH of 9.00. Moreover, except at the initial stage, the sudden decline of water flux (meaning the occurrence of severe membrane fouling) occurred in two conditions: 1. 0.5 mmol/L Ca^{2+}, active layer facing draw solution (AL-DS) and 1.5 mol/L NaCl (DS); 2. No Ca^{2+}, active layer-facing FS (AL-FS) and 4 mol/L NaCl (DS). This demonstrated that cake layer compaction or pore blocking occurred only when enough foulants were absorbed into the membrane surface, and the water permeation was high enough to compact the deposit inside the porous substrate. Furthermore, bovine serum albumin (BSA) was selected as a co-foulant. The water flux of both co-foulants was between the fluxes obtained separately for the two foulants at pH 3.56, and larger than the two values at pH 9.00. This manifested that, at pH 3.56, BSA alleviated the effect of the cake layer caused by OA, and OA enhanced BSA fouling simultaneously; while at pH 9.00, the mutual effects of OA and BSA eased the membrane fouling.

Introduction

Exploring novel energy-conserving technologies to produce clean water has become increasingly important due to water scarcity and resource depletion (Shannon et al., 2008). As one of the most popular alternative membrane-based technologies, forward osmosis (FO) has aroused great attention around the world over the past few years in a wide range of potential applications including seawater desalination, wastewater reclamation, industrial wastewater treatment and power generation (Achilli et al., 2009; Chung et al., 2012a, 2012b; Hickenbottom et al., 2013; Li et al., 2012). FO utilizes the osmotic pressure difference to drive the permeation of water from a less concentrated feed solution (FS) to a highly concentrated draw solution (DS) across a selectively semi-permeable membrane. Unlike typical pressure-driven membrane processes, FO occurs spontaneously in the absence of hydraulic pressure, and has several advantages, including low fouling potential, high recovery, simplicity, and reliability (Chung et al., 2012a, 2012b; Hoover et al., 2011; Zhao et al.,

* *Corresponding author*. E-mail: qyyue58@aliyun.com (Qinyan Yue).

http://dx.doi.org/10.1016/j.jes.2016.02.008

2012). Moreover, the FO process where a draw solution recovery process is not required is low energy consuming.

At the same time, there are some challenging factors hindering the advance of the FO process, such as the need for better membranes and draw solutes, concentration polarization (CP) and membrane fouling. As a membrane process, the FO process of course cannot be an exception to being vulnerable to the enduring problem of membrane fouling. Solutes or particles in the solution lead to fouling by depositing onto surfaces or into pores of the membrane. Membrane fouling has multifarious adverse impacts including decreasing water flux, deteriorating product water quality, and increasing maintenance burden, depending on its severity. There have been a few works targeting FO membrane fouling. For instance, Mi and Elimelech (2010) compared the fouling behaviors of three different foulants: bovine serum albumin (BSA), humic acid and alginate. Liu and Mi (2012) investigated the combined fouling by organic and inorganic foulants in FO membrane processes, and observed the synergistic effect between alginate fouling and gypsum scaling in a combined fouling experiment. Boo et al. (2012) investigated colloidal fouling in FO, and observed that reverse salt diffusion was a key factor to control colloidal fouling behavior as well as fouling reversibility. Lee et al. (2010) demonstrated that reverse diffusion of salt from the draw to the feed side exacerbated the cake-enhanced osmotic pressure within the fouling layer. Membrane fouling hinders the further advance of the FO process. To enhance FO performance, more studies should be conducted to provide detailed information on the mechanism and influencing factors of fouling.

Fatty acids are generally present in wastewater effluents due to both natural and anthropogenic sources, such as dairy processing and fermentation plants. Fatty acid has been reported to cause severe membrane fouling in reverse osmosis and ultrafiltration processes (Ang and Elimelech, 2008; Brinck et al., 2000; Priyananda and Chen, 2006). However, despite the ubiquity of fatty acids in wastewater effluents, there have been no investigations on FO membrane fouling caused by fatty acids. In this study, octanoic acid (OA) was selected to represent fatty acids in effluent organic matter due to its solubility in water and potential applications in food supplements. The main objective of this paper was to investigate the influence of OA on membrane fouling in the FO process. The influences of FS chemistry (solution pH, calcium concentration and occurrence of BSA, which was selected as an organic co-foulant to represent proteins), initial permeate flux and membrane orientation were determined in terms of water flux. Moreover, the effect of fouling behavior on the reverse draw solute diffusion was also evaluated. This research could provide some theoretical support and application reference for future works about fatty acid fouling in the FO process, and fill a gap in existing research.

1. Materials and methods

1.1. Organic foulant

OA (min 99% pure) was obtained from Kermel Company in Tianjin, China. Its molecular weight is 144.21. The concentration of OA used in the fouling test was 4.7 mmol/L, which was the saturation concentration of OA at 20°C. To achieve the intended OA concentration, 3.2 mL OA was dissolved in 1 L FS for at least 8 hr prior to use (Ang and Elimelech, 2008).

BSA (Klontech Company from Roche) was chosen as a model protein due to its ready availability, fat binding properties and structure. The properties were as follows: molecular weight approximately 68 kDa; purity greater than 96%; water content less than 5%; isoelectric point pH 4.7. A stock solution of BSA (2 g/L) was prepared by dissolving the organic foulant (received in powder form) in deionized (DI) water and mixing for over 12 hr to ensure complete dissolution. The stock solution was stored in sterilized glass bottles at 4°C without further purification (Ang and Elimelech, 2007).

1.2. Test solutions

For fouling experiments, the FS contained 10 mmol/L NaCl and some foulants (4.7 mmol/L OA and/or 200 mg/L BSA). The pH was adjusted using 1 mol/L NaOH. The DS was composed of 1.5 or 4 mol/L NaCl. The osmotic pressures of 10 mmol/L NaCl feed and 1.5 or 4 mol/L NaCl draw solutions were predicted using an OLI Systems analyzer and determined to be 0.359 and 73.5/234.2 bar, respectively. Moreover, calcium chloride (100 mmol/L) stock solution was used to achieve the desired solution chemistry to investigate the effect of Ca^{2+} concentration on OA fouling.

1.3. FO membrane

The commercial flat-sheet cellulose triacetate (CTA) FO membrane used in this study was provided by Hydration Technology Innovations (HTI), Albany, USA. It is made from cellulose acetate embedded in a polyester woven mesh, which has been used widely in FO processes for wastewater reclamation and seawater desalination (Jin et al., 2012). Properties of the CTA FO membrane are as follows: The contact angles of the active layer and support layer are 76.6° and 81.8°, indicating that the membrane is relatively hydrophilic. The zeta potential of the active layer at pH 6 is −2.1 mV, which manifests that the membrane is negatively charged. Furthermore, the pure water permeability coefficient was measured under reverse osmosis orientation and determined to be 0.98 L/(m^2·hr·bar).

Given the absence of hydraulic pressure in the FO process, there are two possible membrane orientations. Specifically, one of the membrane orientations is referred to as the active layer facing draw solution (AL-DS) orientation, in which DS was placed against the active layer and FS faced the support layer. It was used in the pressure-retarded osmosis process, since the porous support layer was required to resist the pressurization of the permeate stream (Lee et al., 1981). The other one is referred to as the AL-FS orientation, which is the typical orientation utilized in FO in previous studies (McCutcheon et al., 2005, 2006).

1.4. Forward osmosis system and fouling experiments

The fouling tests were conducted using a bench scale flat-sheet cross-flow FO system, which was similar to the unit used in our earlier study (Zhao et al., 2015). It contained a flat membrane sheet placed in a rectangular channel with

internal dimensions of 7.7 cm long, 2.6 cm wide and 0.3 cm high. To obtain different initial fluxes, 1.5 mol/L and 4 mol/L NaCl were employed as DS. A weighing balance (Sartorius weighing technology GmbH, Gottingen, Germany) was used to record the variation in the DS weight for water flux computation.

For the experimental protocol, the membrane was immersed in DI water for 12 hr. Then, 1 L FS with foulant and 1 L DS were added to the feed and draw tank, respectively. After reaching the desired temperature of 25°C, the bypass valves of both cross-flows were closed to allow flow of FS and DS through both sides of the membrane. The cross-flow velocities for both the feed and draw sides were fixed at 8.5 cm/sec. The fouling experiment lasted 12 hr. The reverse salt diffusion was obtained by measuring the total dissolvable solid in FS using a conductivity meter from Mettler–Toledo. Baseline experiments were carried out in the absence of the foulant in FS, in which the other conditions were the same as the fouling experiments.

In the fouling experiments, the water flux declined for two main reasons: one was the lower osmotic pressure due to the dilution of DS and concentration of FS; the other one was membrane fouling, which was made up of three parts (CP, cake layer and pore blocking) (Kimura et al., 2000). It is worth mentioning that the effect of CP on the water permeation was prominent. The experimental flux was much less than the theoretical value mainly due to the negative effect of CP. The CP effect occurred in all the FO processes including the baseline experiments. In the AL-DS orientation, water is diffused from the feed to the draw side, resulting in dilutive external CP (ECP) in the active layer and concentrative internal CP (ICP) in the porous support layer, while in the AL-FS orientation, dilutive ICP and concentrative ECP occur in the porous support layer and active layer, respectively. The CP effect increases the concentration of the feed side near the membrane surface, while it decreases the concentration of the draw side. The formation of a cake layer is common in membrane processes, including a loose layer and a compact layer. Pore blocking is the most severe type of fouling in the membrane process, which is hard to clean up.

Baseline experiments were conducted to quantify the declined flux resulted from the decreased osmotic pressure due to the dilution of DS and concentration of FS, and the CP effect, in order to investigate the effect of the cake layer and pore blocking on the water flux. First, the baseline flux was divided by its corresponding initial flux to obtain a normalization factor. Then the normalization factor was subtracted from the flux data from the fouling experiment to obtain the corrected flux.

2. Results and discussion

2.1. Influence of solution chemistry on water permeation

2.1.1. Effect of solution pH

The solution pH plays a major role in the characteristics of OA molecules. To be specific, at solution pH below the pKa value of OA (4.9), dissolved OA molecules behave like hydrophobic uncharged molecules, which are largely undissociated; while at elevated solution pH above the pKa value of OA, the OA molecules are fully dissociated and behave as anionic surfactants. The unadjusted solution pH (3.56) and an elevated solution pH (9.00) were chosen to determine the effect of pH on OA fouling of FO membrane. The amount of undissociated OA was larger than 90% and less than 10% at pH 3.56 and 9.00, respectively (Brinck et al., 2000). As can be seen in Fig. 1, there were significant differences in the flux reduction at different solution pH values. The baseline experiments were tested in the absence of the foulant in FS. Water flux declined from 15.00 to 12.59 L/(m^2·hr) (LMH) over 12 hr in the baseline experiment, which was only affected by the dilution of DS and CP. The water flux of the fouling test at pH 3.56 was much less than that of the baseline, while the flux at pH 9.0 was slightly higher than that of the baseline. This was mainly attributed to the different characteristics of OA molecules at different solution pH levels. Most of the OA molecules were undissociated and uncharged at pH 3.56, and they easily became attached to the membrane surface and made the membrane more hydrophobic, resulting in water flux decline. As the adsorption sites of the membrane were limited, the adsorption process was rapid and reached adsorption equilibrium in the initial 0.5 hr. Moreover, the undissociated OA molecules combined with each other easily and formed a cake layer or gel layer, which lowered the water permeation in two ways: (1). The cake layer increased the resistance of water diffusion from the feed to the draw side; (2). Some draw solutes permeated from the draw to the feed side. These salts accumulated on the membrane surface in the feed side, causing blockage of the cake layer, and enhanced the osmotic pressure of the feed side.

On the other hand, as pH increased above the pKa value after addition of NaOH, OA molecules were fully dissociated and behaved as anionic surfactants. The OA and membrane surface were both negatively charged and repelled each other, which alleviated the accumulation of OA molecules and avoided the formation of the gel layer. Furthermore, anionic

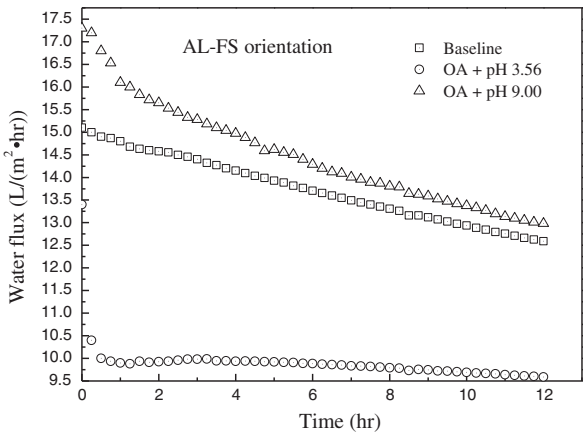

Fig. 1 – Effect of solution pH on octanoic acid (OA) fouling of the commercial flat-sheet cellulose triacetate FO (CTA-FO) membrane. Feed solution (FS) contained 4.7 mmol/L OA and 10 mmol/L NaCl, and its pH was adjusted by adding NaOH stock solution (0.1 mol/L). Other test conditions: Draw solution (DS) initially containing 1.5 mol/L NaCl, AL-FS orientation, cross-flow velocity of 8.5 cm/sec, and temperature of 25 ± 1°C. AL-FS: active layer-facing FS.

surfactants can enhance the surface hydrophilicity of a membrane to some extent at some certain concentrations, and then promote water permeation (Zhao et al., 2015).

2.1.2. Effect of Ca^{2+} concentration

As a major divalent cation, Ca^{2+} exists extensively in natural and wastewaters. The effect of Ca^{2+} concentration on water flux was investigated in the presence of OA. The experiments were conducted in both the AL-FS and AL-DS orientations and the results are shown in Fig. 2. For the baseline, the water flux of AL-DS was higher than that of AL-FS orientation, due to the fact that the ICP in the AL-FS orientation was more severe than that in the AL-DS orientation. However, the decline of water flux in the AL-DS orientation was faster than that in the AL-FS orientation, which was attributed to the self-compensation of ICP at the draw side in the AL-FS orientation (Tang et al., 2010). In the fouling test, the water permeation in the presence of Ca^{2+} was higher than that in the absence of Ca^{2+} in the AL-FS orientation. Moreover, the water permeation increased with the concentration of Ca^{2+}. As we know, the membrane surface was negatively charged, and the OA acted as hydrophobic uncharged molecules at unadjusted solution pH (3.56). In the absence of Ca^{2+}, the OA molecules were prone to attach onto the membrane surface and form a gel layer, resulting in the water flux declining. However, in the presence of Ca^{2+}, Ca^{2+} and OA molecules would compete against each other for the limited sites on the membrane surface. Moreover, the OA and calcium formed a-OA complexes and assembled micelle-like structures, which had the hydrophilic ends containing calcium facing the bulk water (Ang and Elimelech, 2008). Upon deposition on the membrane surface, the Ca-OA complexes coated some adsorption sites for the OA molecules.

In the AL-DS orientation, the variation of the water flux for 0.5 mmol/L Ca^{2+} was peculiar. It has been reported that the ICP and ECP forms very soon in the beginning of the test, while the cake layer or pore blocking usually occurs in the subsequent phase (McCutcheon and Elimelech, 2006). The water flux of 0.5 mmol/L Ca^{2+} declined significantly in the 5th hr, indicating that compaction of the cake layer or pore blocking occurred. This might be because the OA molecules and Ca-OA complexes deposited onto the membrane surface and were compacted by the high water permeation, leading to pore blocking of the porous support substrate (Mi and Elimelech, 2008). A sudden decline did not occur in the presence of 2 mmol/L Ca^{2+}, which was mainly due to the fact that Ca^{2+} ions occupied most adsorption sites on the membrane surface. On the other hand, a significant change did not occur in the absence of Ca^{2+}, perhaps because the water permeation was too low to compact the OA foulant layer.

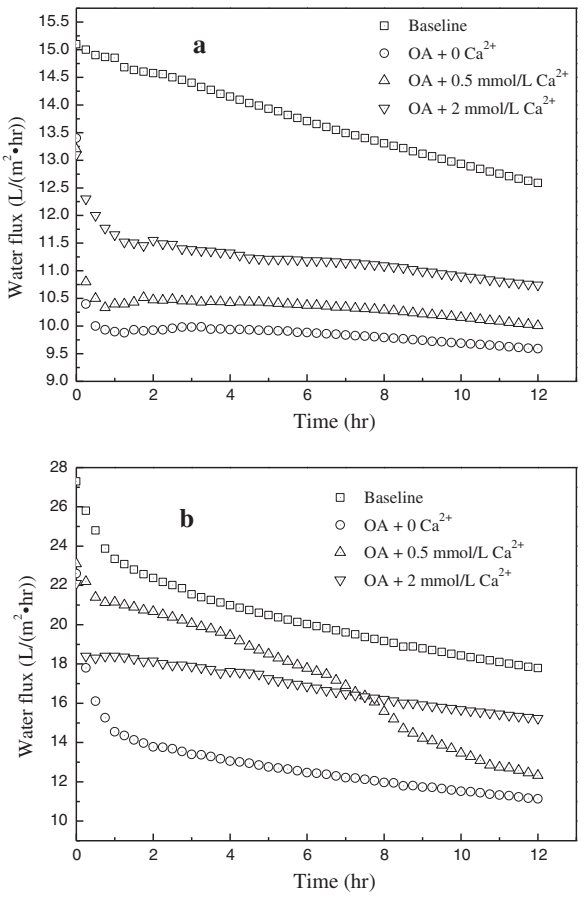

Fig. 2 – Effect of calcium concentration on OA fouling of the CTA-FO membrane (a) in the active layer facing the FS (AL-FS) orientation and (b) in the active layer facing the DS (AL-DS) orientation. Total ionic strength of the FS was fixed at 10 mmol/L by varying NaCl and Ca^{2+} concentration. pH was 3.56. Other test conditions: DS initially containing 1.5 mol/L NaCl, AL-FS orientation, cross-flow velocity of 8.5 cm/sec, and temperature of 25 ± 1°C.

2.2. Effect of membrane orientation on fouling

Since there are many differences in performance between the AL-FS and AL-DS orientations, fouling tests for both AL-FS and AL-DS orientations were conducted for comparison. The concentrations of DS (NaCl solution) used in AL-FS and AL-DS orientations were 4 and 1.5 mol/L respectively to obtain the same initial flux. As shown in Fig. 3, for the baseline, the water flux of the AL-FS orientation declined more slowly than that of the AL-DS orientation, which had been reported in Section 2.1.2. Hydrodynamic interactions, such as permeation drag and shear force, will control the membrane fouling behavior by influencing the deposition and accumulation of foulant molecules on the membrane surface (Xu et al., 2010). In the pores of the porous support layer, the effect of hydrodynamic shear forces is weakened greatly. Consequently, in the fouling test, the flux of the AL-DS orientation declined significantly in the initial stage, which was mainly due to the formation of CP and the gel layer in the porous support layer. In the subsequent phase, the water flux went down smoothly, indicating that gel layer did not deteriorate further. On the other hand, the flux of the AL-FS orientation declined significantly in the initial 0.5 hr, declined relatively smoothly from the 0.5th to the 4th hr, and then had another dramatic decline. This indicated that the compaction of the cake layer or pore blocking occurred at the 4th hr. The fact that this condition did not occur in the condition of the AL-DS orientation showed that even though sufficient OA molecules

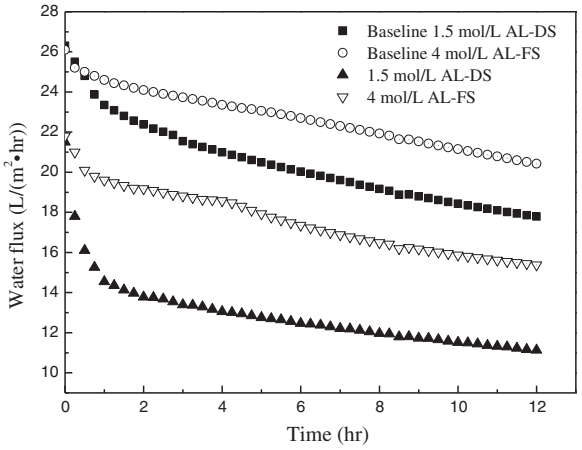

Fig. 3 – Effect of membrane orientation on OA fouling of the CTA-FO membrane. The draw solution contained 4 mol/L NaCl for the AL-FS orientation and 1.5 mol/L NaCl for the AL-DS orientation. Other test conditions: DS initially containing 1.5 mol/L NaCl, AL-FS orientation, cross-flow velocity of 8.5 cm/sec, and temperature of 25 ± 1°C.

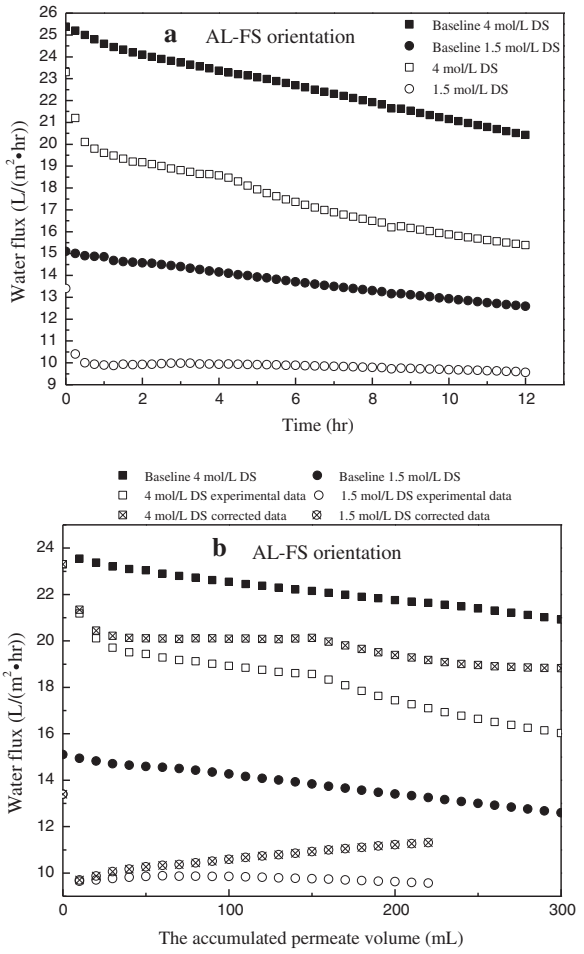

Fig. 4 – Effect of initial permeate flux on OA fouling of the CTA-FO membrane (a) water flux vs time; (b) water flux vs accumulated permeate volume. 1.5 mol/L and 4 mol/L NaCl solutions were chosen as draw solutions to obtain different initial permeate fluxes. Other test conditions: DS initially containing 1.5 mol/L NaCl, AL-FS orientation, cross-flow velocity of 8.5 cm/sec, and temperature of 25 ± 1°C.

had been absorbed into the membrane surface, compaction of the cake layer or pore blocking would not occur when the water flux was low.

2.3. Effect of initial permeate flux on fouling

The effect of initial permeate flux on fatty acid fouling of the FO membrane was investigated in the AL-FS orientation. As revealed in Fig. 4a, for the baseline, the water flux declined gradually with time during the whole process. However, in the fouling test, the water flux of 1.5 mol/L DS declined significantly in the initial time (0.5 hr); and the flux of 4 mol/L DS declined rapidly in the initial time (0.5 hr) and at the 4th hr. It has been proven that the effect of initial flux on membrane fouling can be mainly attributed to permeation drag resulting from convective flow toward the membrane (Ang and Elimelech, 2008). The permeation drag led to the formation of a cake layer. Once the cake layer formed, fouling became much less sensitive to changes in hydrodynamic conditions. At low membrane flux, a loose cake layer formed in the initial stage, and then tended to maintain a dynamic balance on the whole. Consequently, the water flux declined in the initial stage, and then remained stable. Unlike low water permeation, high water permeation had the power to transform the fouling layer from loose to compact (Mi and Elimelech, 2008).

To prove and bolster the above claim, the curves of permeate flux decline as a function of accumulated permeate volume were calculated and presented in Fig. 4b. Because the water flux of 1.5 mol/L was low in the fouling test, the data only extended to the accumulated permeate volume of 220 mL. Instead of the actual observed flux, the corrected flux was used in the flux decline curves of the fouling experiments, which eliminated the effects of the dilution of DS and the baseline CP effect. The corrected flux solely represented the effect of the cake layer and pore blocking. For the case of 4 mol/L DS, the water flux declined at two points: the formation of a cake layer at 0.25 hr; and the onset of compaction of the cake layer and pore blocking at the 4th hr. For the case of 1.5 mol/L DS, the corrected flux only declined in the initial time period due to the formation of the cake layer, which was consistent with the above analysis.

On the other hand, there is an interesting phenomenon in Fig. 4b. For the case of 1.5 mol/L DS, the corrected flux increased from the permeate volume 40 mL on. As we all know, the corrected water flux separated the effect of dilution of DS and the effect of baseline CP. When the water permeated from the feed to the draw side, the ICP was enhanced in the support layer on the draw side. The water permeation of the 1.5 mol/L DS fouling test was much less than that of the baseline, and thus, compared with the baseline, the passive role of ICP was weakened in the fouling test. Therefore, the corrected flux increased after the cake layer reached stability. However, in the case of 4 mol/L DS, the corrected flux kept in

relative balance during the test with the exception of the two sudden drops. Though the passive role of ICP was weakened, the increase in the corrected flux was not obvious. This was perhaps due to a gradual increase in the resistance of the cake layer due to the high water permeation.

2.4. Effect of feed foulant composition on fouling

In reality, there are various foulant types present in wastewater effluents. Each foulant type has different fouling potentials on the FO membranes. The interaction of foulants can take various forms, which will change the physical (size and molecular weight) and chemical (charge and hydrophobicity) characteristics of the combined foulants. It is difficult to understand the FO membrane fouling mechanisms in wastewater reclamation because the physical and chemical interactions among the various types of foulants are extremely complicated. An approach to minimize such complexity would be to restrict the types of foulants in an initial study and then to increase the number of foulant types in a follow-up study.

In this study, BSA was selected to represent protein in secondary wastewater effluent. To study the mutual effects of co-existing OA and BSA on the water permeation of the FO membrane, tests were carried out with feed solutions containing 200 mg/L BSA or/and 4.7 mmol/L OA at pH of 3.56 and 9.00. As described in Fig. 5, at solution pH 3.56, the water flux in the presence of BSA was higher than that in the presence of OA. In addition, the water flux in the presence of BSA declined gradually, while the flux in the presence of OA remained relatively stable. In the presence of both co-foulants, the membrane flux was between that of the two separate cases, manifesting that BSA alleviated the fatty acid fouling. At solution pH 3.56, fatty acids were largely undissociated and tended to combine with each other and form the gel layer, resulting in low water permeation. BSA molecules repelled each other, and then gradually attached to the active layer of the membrane, making the flux decline gradually. When both OA and BSA appeared, the deposition of BSA on the membrane surface could coat some adsorption sites for the fatty acid, mitigating the effect of the cake layer (Ho and Zydney, 1999, 2000). On the other hand, at solution pH 9.00, the membrane flux in the presence of both co-foulants was higher than both of the two separate cases at the end of the fouling run. This showed that fatty acid and BSA would react with each other and that the mutual effects eased the membrane fouling. At solution pH 9.00, BSA was negatively charged, and the fatty acid salt acted as an anionic surfactant. The electrostatic repulsion among the membrane surface, BSA and OA reduced the fouling of the membrane and increased the permeate flux.

2.5. Influence of fouling on reverse salt flux

In order to better evaluate FO performance, the rejection of draw solutes was measured in terms of reverse diffusion of draw solutes or reverse solute flux (RSF). The reverse salt permeation from the DS to FS would not only contaminate the feed stream but also increase the replenishment cost of the draw solute. The fouling layer has been reported to have some influence on the RSF. It was therefore relevant to study reverse salt diffusion during the fouling test, and the results are shown in Fig. 6. The 0 on the vertical axis represents the average RSF of the CTA-FO membrane measured at the start of the fouling tests. There was little difference between the RSF values at the start of different fouling tests. In addition, 1–6 represent the RSF values measured at the end of the fouling test under different conditions. In both the AL-DS and AL-FS orientations, RSF at the end of fouling was less than that during the start of fouling (about 67 gMH in the AL-DS orientation and 39 gMH in the AL-FS orientation), implying the major effect of the fouling layer on Na^+ rejection. It can be inferred that the fouling layer formed on the membrane surface would act like an additional 'barrier' to reduce Na^+ diffusivity through the membrane. Moreover, although the fouling in the AL-DS orientation was more severe than that in the AL-FS orientation, the RSF of the AL-DS orientation was higher than that of the AL-FS orientation. This has been studied by some previous researchers, which was mainly

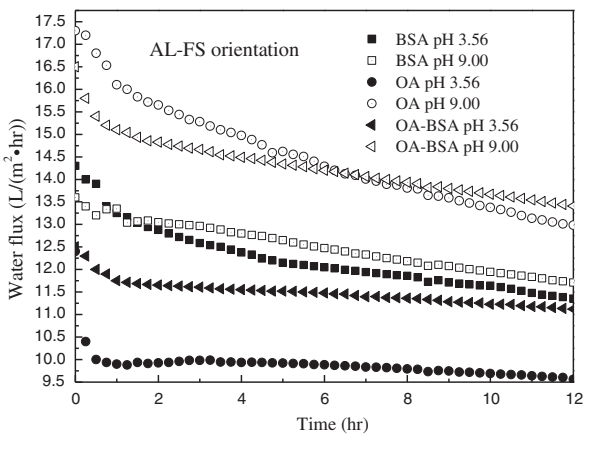

Fig. 5 – Mutual effect of co-existence of OA and BSA on OA fouling. Test conditions: DS initially containing 1.5 mol/L NaCl, AL-FS orientation, cross-flow velocity of 8.5 cm/sec, and temperature of 25 ± 1°C.

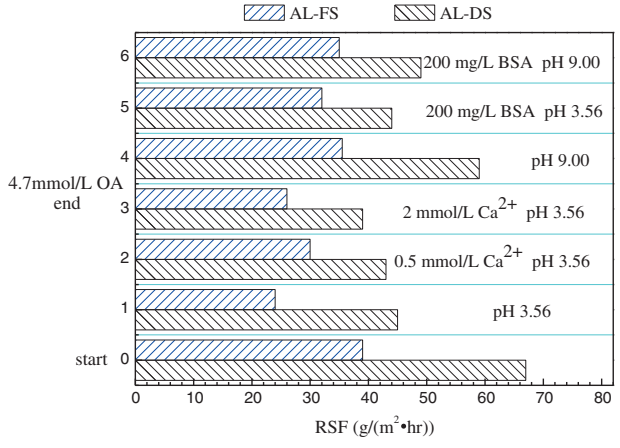

Fig. 6 – Sodium ion rejection of CTA-FO membranes measured at the start and end of fouling runs at an unadjusted and elevated feed solution pH of 3.56 and 9.00, respectively. 1–6 represent the RSF values measured at the end of the fouling test under different conditions.

attributed to the effect of CP (Chanukya et al., 2013; Phillip et al., 2010; Tan and Ng, 2013; Tang et al., 2010).

3. Conclusions

This study concentrated on the membrane fouling mechanisms of fatty acids during the FO process. OA was chosen as a representative fatty acid in secondary wastewater effluent. The water flux–decline curves were obtained under different scenarios of FS chemistry (solution pH and Ca^{2+} concentration), initial permeate flux, membrane orientation, and co-existence with BSA.

In the presence of the foulant OA, the water permeation was enhanced at pH 9.00, while it was restrained at pH 3.56. At pH 9.00, some adsorbed OA anions on hydrophobic patches of the membrane made the membrane more hydrophilic, increasing the water flux. At pH 3.56, the OA molecules easily combined with each other and then attached to the membrane surface, forming a gel layer. The water flux increased with increasing Ca^{2+} concentration in the AL-FS orientation. Ca^{2+} and OA molecules would compete against each other in attaching onto the limited sites on the membrane surface, restraining the formation of a cake layer. The compaction of the cake layer or pore blocking occurred in the 5th hr in the condition of 0.5 mmol/L Ca^{2+} in the AL-DS orientation using 1.5 mol/L NaCl as DS; while it did not occur in the condition of 0 and 2 mmol/L Ca^{2+}. Moreover, cake layer compaction or pore blocking formed in the 4th hr in the AL-FS orientation using 4 mol/L NaCl as DS. This indicated that cake layer compaction or pore blocking occurred only in very special cases: (1) Enough foulants attached on the membrane surface; (2) High water permeation providing the force to push foulant deposits into the porous support substrate. High permeate flux could induce the transition of the fouling layer from a looser structure to a much more compact cake layer, making the membrane fouling more severe.

The effect of OA on membrane fouling with BSA was also studied to investigate the implications of OA fouling for waste-water reclamation. At solution pH 3.56, the membrane flux in the presence of both co-foulants was higher than that of OA, and lower than that of BSA, indicating that BSA alleviated the fouling caused by the fatty acid. In contrast, at solution pH 9.00, the membrane flux in the presence of both co-foulants was higher than both of the two separate cases at the end of the fouling run. This showed that fatty acid and BSA would react with each other and that the mutual effect would mitigate the membrane fouling. In addition, the fouling layer formed on the membrane surface acted like an additional barrier by reducing Na^{+} diffusivity across the membrane.

REFERENCES

Achilli, A., Cath, T.Y., Childress, A.E., 2009. Power generation with pressure retarded osmosis: An experimental and theoretical investigation. J. Membr. Sci. 343 (1), 42–52.

Ang, W.S., Elimelech, M., 2007. Protein (BSA) fouling of reverse osmosis membranes: Implications for wastewater reclamation. J. Membr. Sci. 296 (1–2), 83–92.

Ang, W.S., Elimelech, M., 2008. Fatty acid fouling of reverse osmosis membranes: Implications for wastewater reclamation. Water Res. 42 (16), 4393–4403.

Boo, C., Lee, S., Elimelech, M., Meng, Z., Hong, S., 2012. Colloidal fouling in forward osmosis: Role of reverse salt diffusion. J. Membr. Sci. 390-391, 277–284.

Brinck, J., Jönsson, A.S., Jönsson, B., Lindau, J., 2000. Influence of pH on the adsorptive fouling of ultrafiltration membranes by fatty acid. J. Membr. Sci. 164 (1), 187–194.

Chanukya, B.S., Patil, S., Rastogi, N.K., 2013. Influence of concentration polarization on flux behavior in forward osmosis during desalination using ammonium bicarbonate. Desalination 312, 39–44.

Chung, T.-S., Li, X., Ong, R.C., Ge, Q., Wang, H., Han, G., 2012a. Emerging forward osmosis (FO) technologies and challenges ahead for clean water and clean energy applications. Curr. Opin. Chem. Eng. 1 (3), 246–257.

Chung, T.-S., Zhang, S., Wang, K.Y., Su, J., Ling, M.M., 2012b. Forward osmosis processes: Yesterday, today and tomorrow. Desalination 287, 78–81.

Hickenbottom, K.L., Hancock, N.T., Hutchings, N.R., Appleton, E.W., Beaudry, E.G., Xu, P., Cath, Tzahi Y., 2013. Forward osmosis treatment of drilling mud and fracturing wastewater from oil and gas operations. Desalination 312, 60–66.

Ho, C.-C., Zydney, A.L., 1999. Effect of membrane morphology on the initial rate of protein fouling during microfiltration. J. Membr. Sci. 155 (2), 261–275.

Ho, C.-C., Zydney, A.L., 2000. A combined pore blockage and cake filtration orientationl for protein fouling during microfiltration. J. Colloid Interface Sci. 232 (2), 389–399.

Hoover, L.A., Phillip, W.A., Tiraferri, A., Yip, N.Y., Elimelech, M., 2011. Forward with osmosis: emerging lications for greater sustainability. Environ. Sci. Technol. 45 (23), 9824–9830.

Jin, X., She, Q., Ang, X., Tang, C.Y., 2012. Removal of boron and arsenic by forward osmosis membrane: Influence of membrane orientation and organic fouling. J. Membr. Sci. 389, 182–187.

Kimura, K., Watanabe, Y., Ohkuma, N., 2000. Filtration resistance and efficient cleaning methods of the membrane with fixed nitrifiers. Water Res. 34 (11), 2895–2904.

Lee, K., Baker, R., Lonsdale, H., 1981. Membranes for power generation by pressure-retarded osmosis. J. Membr. Sci. 8 (2), 141–171.

Lee, S., Boo, C., Elimelech, M., Hong, S., 2010. Comparison of fouling behavior in forward osmosis (FO) and reverse osmosis (RO). J. Membr. Sci. 365 (1–2), 34–39.

Li, Z.Y., Yangali-Quintanilla, V., Valladares-Linares, R., Li, Q., Zhan, T., Amy, G., 2012. Flux patterns and membrane fouling propensity during desalination of seawater by forward osmosis. Water Res. 46 (1), 195–204.

Liu, Y., Mi, B., 2012. Combined fouling of forward osmosis membranes: Synergistic foulant interaction and direct observation of fouling layer formation. J. Membr. Sci. 407-408, 136–144.

McCutcheon, J.R., Elimelech, M., 2006. Influence of concentrative and dilutive internal concentration polarization on flux behavior in forward osmosis. J. Membr. Sci. 284 (1–2), 237–247.

McCutcheon, J.R., McGinnis, R.L., Elimelech, M., 2005. A novel ammonia–carbon dioxide forward (direct) osmosis desalination process. Desalination 174 (1), 1–11.

McCutcheon, J.R., McGinnis, R.L., Elimelech, M., 2006. Desalination by ammonia–carbon dioxide forward osmosis: Influence of draw and feed solution concentrations on process performance. J. Membr. Sci. 278 (1), 114–123.

Mi, B., Elimelech, M., 2008. Chemical and physical aspects of organic fouling of forward osmosis membranes. J. Membr. Sci. 320 (1–2), 292–302.

Mi, B., Elimelech, M., 2010. Organic fouling of forward osmosis membranes: Fouling reversibility and cleaning without chemical reagents. J. Membr. Sci. 348 (1–2), 337–345.

Phillip, W.A., Yong, J.S., Elimelech, M., 2010. Reverse draw solute permeation in forward osmosis: Modeling and experiments. Environ. Sci. Technol. 44 (13), 5170–5176.
Priyananda, P., Chen, V., 2006. Flux decline during ultrafiltration of protein-fatty acid mixtures. J. Membr. Sci. 273 (1–2), 58–67.
Shannon, M.A., Bohn, P.W., Elimelech, M., Georgiadis, J.G., Marinas, B.J., Mayes, A.M., 2008. Science and technology for water purification in the coming decades. Nature 452 (7185), 301–310.
Tan, C.H., Ng, H.Y., 2013. Revised external and internal concentration polarization models to improve flux prediction in forward osmosis process. Desalination 309, 125–140.
Tang, C.Y., She, Q., Lay, W.C.L., Wang, R., Fane, A.G., 2010. Coupled effects of internal concentration polarization and fouling on flux behavior of forward osmosis membranes during humic acid filtration. J. Membr. Sci. 354 (1–2), 123–133.
Xu, Y., Peng, X., Tang, C.Y., Fu, Q.S., Nie, S., 2010. Effect of draw solution concentration and operating conditions on forward osmosis and pressure retarded osmosis performance in a spiral wound module. J. Membr. Sci. 348 (1), 298–309.
Zhao, S., Zou, L., Tang, C.Y., Mulcahy, D., 2012. Recent developments in forward osmosis: Opportunities and challenges. J. Membr. Sci. 396, 1–21.
Zhao, P., Gao, B., Yue, Q., Shon, H.K., 2015. The performance of forward osmosis process in treating the surfactant wastewater: the rejection of surfactant, water flux and physical cleaning effectiveness. Chem. Eng. J. 281, 688–695.